

# A comprehensive study of 94 open clusters based on the data from IPHAS, GAIA DR2, and other sky surveys

L. N. Yalyalieva,<sup>1,2,\*</sup> A. A. Chemel,<sup>2</sup> E. V. Glushkova,<sup>1,2,†</sup> A. K. Dambis,<sup>1,‡</sup> and A. D. Klinichev<sup>2</sup>

<sup>1</sup>*Sternberg Astronomical Institute, M. V. Lomonosov Moscow State University, Universitetskii pr. 13, Moscow, 119992 Russia*

<sup>2</sup>*Lomonosov Moscow State University, Faculty of Physics,  
1, bld.2, Leninskie Gory, Moscow, 119992, Russia*

We determine the color excesses, photometric distances, ages, astrometric parallaxes and proper motions for 94 open clusters in the northern part of the Milky Way. We estimate the color excesses and photometric distances based on the data from IPHAS photometric survey of the northern Galactic plane using individual total-to-selective extinction ratios  $R_r = A_r/E_{r-i}$  for each cluster computed via the color-difference method based on IPHAS  $r$ ,  $i$ , and  $H_\alpha$ -band, 2MASS  $J$ ,  $H$ , and  $K_s$ -band, WISE  $W1$ -band, and Pan-STARRS  $i$ ,  $z$ , and  $y$ -band data. The inferred  $R_r$  values vary significantly from cluster to cluster spanning the  $R_r = 3.1$ – $5.2$  interval with a mean and standard deviation equal to  $\langle R_r \rangle = 3.99$  and  $\sigma R_r = 0.34$ , respectively. We identified cluster members using (1) absolute proper motions determined from individual-epoch positions of stars retrieved from IPHAS, 2MASS, URAT1, ALLWISE, UCAC5, and Gaia DR1 catalogs and positions of stars on individual Palomar Sky Survey plates reconstructed based on the data provided in USNO-B1.0 catalog and (2) absolute proper motions provided in Gaia DR2 catalog, and computed the average Gaia DR2 trigonometric parallaxes and proper motions of the clusters. The mean formal error of the inferred astrometric parallaxes of clusters is of about 7 microarcseconds, however, a comparison of astrometric and photometric parallaxes of our cluster sample implies that Gaia DR2 parallaxes are, on the average, systematically underestimated by  $45 \pm 9$  microarcseconds. This result agrees with estimates obtained by other authors using other objects. At the same time, we find our photometric distance scale to be correct within the quoted errors (the inferred correction factor is equal to unity to within a standard error of 0.025).

## I. INTRODUCTION

The number of sky surveys providing various data about the properties of a huge number of objects has increased substantially in recent decades. When using photometric catalogs most of the researchers employ them only as sources of star magnitudes in various passbands. However, all such catalogs also contain equatorial coordinates of the objects, which can be used for computing both relative and absolute proper motions of stars over a long time interval, which is especially important for binary systems. A recent study by Chemel et al. [1] represents a successful case of the use of six major sky surveys for determining absolute proper motions of 115 Galactic globular clusters.

In this study we attempt to determine the proper motions of stars using position data from seven photometric sky surveys in the neighborhood of Galactic open clusters observed within the framework of IPHAS survey [2, 3]. We do it to identify cluster members and apply to them the algorithm for estimating the basic open cluster parameters via a modified Q-method as described by Dambis et al. [4]. Although young open clusters are the most suitable Galactic disk tracers, their basic parameters (distances, ages, and color excesses) still needs to be

refined. One of the two most popular sources of information about open cluster parameters - the catalog of Dias et al. [5] is a compilation and contains the data of various accuracy and reliability for about 2000 objects. Although the authors of another data source - Kharchenko et al. [6] - determined the parameters of more than 3000 clusters by applying the same technique to 2MASS photometry [7], their estimates are reliable only for nearby and old clusters whose Hertzsprung–Russel diagrams show a conspicuous clump at the base of the red giant branch. For all other open clusters the parameter estimates based on relatively shallow  $J, H, K_S$  photometry is unreliable and this especially concerns distances, which are determined by fitting an isochrone to the Hertzsprung–Russel diagram, because for the photometric bands considered the main sequence is practically vertical for young clusters located beyond 1 kpc.

In the context of this study of special interest is investigation of the extinction law toward each cluster and a comparison of the average cluster parallaxes inferred from GAIA DR2 data [8, 9] with the corresponding photometric parallaxes determined from IPHAS photometry [2, 3].

---

\*Electronic address: yalyalieva@yandex.ru

†Electronic address: elena.glushkova@gmail.com

‡Electronic address: dambis@yandex.ru

## II. EXTRACTION OF CLUSTER DATA FROM CATALOGS

### A. Color excess, distance, and age

We estimate the physical parameters of clusters (color excesses, heliocentric distances, and ages) from Sloan  $r$ - and  $i$ -band and narrow-band  $H_\alpha$  photometry from IPHAS catalog [2, 3]. This survey, which was carried out on the 2.5m Isaac Newton Telescope (INT) in the northern part of the sky, covers the Galactic longitudes  $l = 30^\circ - 215^\circ$  and latitudes  $|b| \leq 5^\circ$  down to a limiting magnitude of 21.2 mag, 20.0 mag, and 20.3 mag in the  $r$ ,  $i$ , and  $H_\alpha$  filters, respectively. Dambis et al. [4] modified the classical  $Q$ -method of Johnson and Morgan [10] and applied it to  $r$ -,  $i$ -, and  $H_\alpha$ -band magnitudes to construct the reddening-free index  $H_\alpha index = (0.755r + 0.245i - H_\alpha)$ . Like in the paper of Dambis et al. [4], here we use the  $(H_\alpha index, r-i)$  diagram to determine the color excess  $E(r-i)$ . The reddening lines in this diagram are parallel to the horizontal axis because the combination  $(0.755r + 0.245i)$  linearly interpolates between the corresponding photometric passbands and sort of imitates a broadband  $H_\alpha$  filter so that  $H_\alpha index$  does not depend on reddening. In the  $(r-i, H_\alpha index)$  diagram Padova PARSEC isochrones [11–13] with ages in the  $\log(t) = 6.0 - 8.5$  interval all have a minimum at the same  $(r-i)$  value and its position is practically independent of metallicity. This is because the strength of  $H_\alpha$  absorption line is the highest in  $A0 - A2$ -type stars. Therefore this method is applicable only to relatively young clusters ( $\log(t) < 8.5$ ) whose main sequences still contain stars of such spectral types. We thus determined the color excess  $E(r-i)$  by shifting the isochrone (at the start we set the age equal to  $\log(t) = 7.2$ ) along the horizontal axis. We then determined the cluster distance modulus from the  $(r-i, r)$ ,  $(H_\alpha index, r)$ , and  $(H_\alpha index, r - 3.98(r-i))$  diagrams and estimated the cluster age only from the  $(r-i, r)$  and  $(H_\alpha index, r - 3.98(r-i))$  diagrams. We adopted the  $r$ - and  $i$ -band magnitudes for stars brighter than  $r = 13$ ,  $i = 12$  from APASS survey [15, 16] and transformed them to the IPHAS photometric system by formulas from [2] because images of these stars are saturated in the IPHAS frames. We described the entire multi-stage procedure in our previous paper [4].

The top left panel in Fig. 1 shows the two-color diagram with the  $\log(t) = 7.59$  isochrone (the thin line) shifted along the horizontal axis by 0.647 to fit the main sequence of the SAI 14 cluster. The thick line shows the same isochrone additionally shifted along the vertical axis to take into account a small systematic zero-point difference between the theoretical isochrones and actually observed sequences. The other three panels in Fig. 1 show isochrones shifted by the distance modulus (the shift in the two lower panels is shown by the dashed lines). The final shift in the two lower panels takes into account the zero-point difference mentioned above.

We estimated all parameters in automatic way using

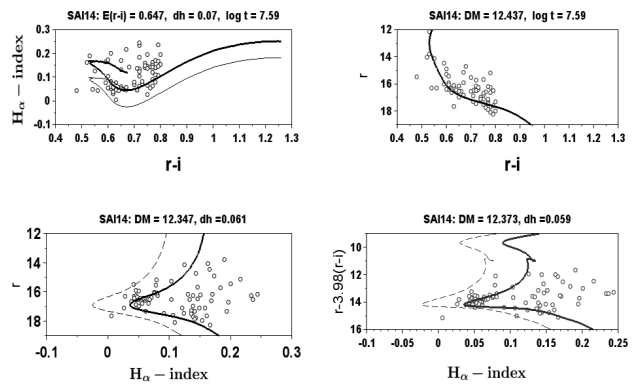


FIG. 1: The  $(r-i, H_\alpha index)$  diagram (top left) and the color-magnitude diagrams  $(r-i, r)$  (top right),  $(H_\alpha index, r)$  (bottom left), and  $(H_\alpha index, r - 3.98(r-i))$  (bottom right) for all stars in the field of SAI 14 cluster within 5 arcmin from its center. The thick solid line shows the  $\log(t) = 7.59$  isochrone shifted in accordance with the inferred color excess and distance modulus. The thin solid or dashed line shows the isochrone before the final shift taking into account the zero-point difference between the theoretical isochrone and observed main sequence of the cluster.

the maximum-likelihood based algorithm proposed by Naylor et al. [17–19] and averaged the distance moduli inferred from three different diagrams.

We determined the distances, color excesses, and ages for 108 open clusters from the catalog of Dias et al. [5], for which the data were available in the IPHAS survey [2, 3] and whose  $(H_\alpha index, r-i)$  showed a minimum.

However, to more confidently estimate the parameters we need to separate cluster members from field stars. To this end we determined the proper motions of stars in the fields of 108 clusters.

### B. Proper motions and cluster membership of stars

To derive proper motions of stars we used the results of major photographic surveys POSS-I, POSS-II, SERC-J, SERC-EJ, ESO-R, AAO-R, SERC-ER, and SERC-I spanning the period from 1949 through 2002 and incorporated into USNO-B1.0 [20] catalog, and the large-scale sky surveys UCAC5 [21] (1998–2004), 2MASS [7] (1997–2001), WISE [22, 23] (2010–2011 with a mean epoch of 2010.5589), URAT1 [24] (2012–2015), IPHAS [2, 3] (2003–2012), and Gaia DR1 [8] (with a mean epoch of 2015.0), which contain sufficiently precise positional data. We first had to cross identify stars over the entire set of catalogs.

We had at our disposal such tools for operating with large astronomical datasets as Aladin interactive sky atlas [25], as well as STILTS [26], TOPCAT [27], and 3 [28] packages. They can be used to perform pairwise or even multiple cross identification of catalogs, but are not very convenient for regular work because the user has each

time to repeat the same sequence of operations (define the set of catalogs employed, cross-match conditions, formats of output files, etc). To simplify this procedure, we developed Crossmatch program, which perform cross-matching of stars over arbitrary set of catalogs in a field of arbitrary radius around the given center, is easy to use and flexible. Crossmatch program is written in java and is available as a jar-file, which can be run from the command line. A substantial part of operations with tables described in Crossmatch algorithm is performed using the capabilities of STILTS program [26]. The source code of the program is available as a single archive file `Crossmatch_4.3.0.zip` at:

[www.sai.msu.ru/groups/cluster/cl/crossmatch/](http://www.sai.msu.ru/groups/cluster/cl/crossmatch/)

We used this program to mutually cross identify the catalogs considered within 30 arcmin from each open cluster with an identification radius of 1 or 2 arcsec. As a result, we obtained up to 13 positions per star. A detailed description of the procedure that we used to compute proper motions can be found in the paper by Chemel et al. [1], which is dedicated to the study of the kinematics of Galactic globular clusters. All proper motions are in the system defined by UCAC5 catalog and the accuracy of individual proper motions is of about 1–2 mas/yr.

We then used the inferred proper motions to identify members of each cluster via the commonly used Sanders’s method [29]. This method allows determining the mean proper motion of cluster and field stars,  $(\mu_\alpha^*, \mu_\delta^*)$  and  $(\mu_\alpha, \mu_\delta)$ , the dispersions of the proper motions of cluster stars –  $(\sigma_\alpha^*, \sigma_\delta^*)$  – and the dispersion of proper motions of field stars,  $(\sigma_\alpha, \sigma_\delta)$ , as well as the fraction of cluster members ( $N$ ). We implemented this method assuming that the velocity distribution of cluster stars is isotropic,  $(\sigma_\alpha^* = \sigma_\delta^* = \sigma^*)$ , and turned the coordinate frame so as to align the axes of the ellipse of the distribution of proper motions of field stars with the coordinate axes.

Probability density functions of cluster members ( $F^*$ ) and field stars ( $F^f$ ) have the following form:

$$F_i^* = \frac{N}{2\pi\sqrt{\sigma^{*2} + \varepsilon_\alpha^{i2}}\sqrt{\sigma^{*2} + \varepsilon_\delta^{i2}}} \cdot \exp\left(-0.5\left[\frac{(\mu_\alpha^i - \mu_\alpha^*)^2}{\sigma^{*2} + \varepsilon_\alpha^{i2}} + \frac{(\mu_\delta^i - \mu_\delta^*)^2}{\sigma^{*2} + \varepsilon_\delta^{i2}}\right]\right) \quad (1)$$

$$F_i^f = \frac{1 - N}{2\pi\sqrt{\sigma_\alpha^2 + \varepsilon_\alpha^{i2}}\sqrt{\sigma_\delta^2 + \varepsilon_\delta^{i2}}} \cdot \exp\left(-0.5\left[\frac{(\mu_\alpha^i - \mu_\alpha)^2}{\sigma_\alpha^2 + \varepsilon_\alpha^{i2}} + \frac{(\mu_\delta^i - \mu_\delta)^2}{\sigma_\delta^2 + \varepsilon_\delta^{i2}}\right]\right), \quad (2)$$

where  $\mu_\alpha^i$  and  $\mu_\delta^i$ ,  $\varepsilon_\alpha^i$ , and  $\varepsilon_\delta^i$  are the proper-motion components and their standard errors for  $i$ th star of the sample. The full probability density function then has the form  $F_i = F_i^* + F_i^f$ .

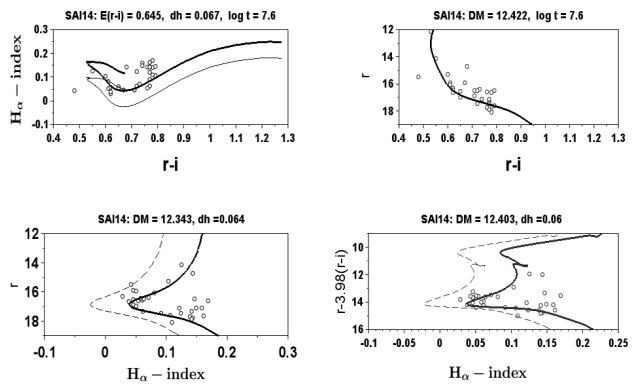


FIG. 2: Color-color diagram and the “color–magnitude diagram” for proper-motion selected cluster members within 5 arcmin from the center of the SAI 14 cluster. The lines are the same as in Fig. 1

The proper motions of individual stars are independent of each other and therefore we compute the likelihood function as the product of probability density functions over all stars of the sample:  $Q = \prod_i F_i$ . In accordance with the maximum likelihood principle we consider the true parameter values to be those corresponding to the most likely distribution, i.e., at the maximum of the likelihood function. In practice, however, it is more convenient to search for the minimum of a function of the following form:

$$L = -\log Q = -\sum_i \log F_i$$

We minimized this function via the conjugate gradient method and estimated the cluster membership probability of each star by the formula:

$$P_i = \frac{F_i^*}{F_i}$$

We then again determined the color excesses, distance moduli, and ages of 108 clusters using the above method and applying it to likely cluster members. Fig. 2 shows the same diagrams as in Fig. 1, but based on SAI 14 cluster members exclusively.

### C. Extinction law

When computing cluster distances one has to take into account interstellar extinction toward the cluster. In most cases the so-called “standard” extinction law of Cardelli et al. [30] or its modification proposed by O’Donnell [31] is used to this end. According to this law extinction is a given function of wavelength and parameter  $R_V$  that is equal to the ratio of extinction in the  $V$  band to the color excess  $E_{B-V}$  ( $R_V = A_V/E_{B-V}$ ),

TABLE I: Filters

Survey	Filter	$\lambda_{eff}, \mu m$
IPHAS	$i$	0.77
	$i$	0.75
	$z$	0.87
Pan-STARSS	$y$	0.96
	$J$	1.25
	$H$	1.65
2MASS	$K_s$	2.17
	$W1$	3.35
WISE	$W1$	3.35

which is supposed to be constant throughout the Galactic disk and equal to  $R_V = 3.1$ . Actually interstellar extinction law (which is in this case determined by the value of parameter  $R_V$ ) varies strongly both with the direction in the Galaxy and with distance [32]. In this paper to characterize extinction law we employ parameter  $R_r$ , which is equal to the ratio of total extinction in IPHAS  $r$  band to the color excess  $E_{r-i}$  ( $R_r = A_r/E_{r-i}$ ), and it is this parameter that we determine for extinction toward each cluster and then use when computing the cluster distances. To study extinction law, we compiled near-infrared photometry in the filters  $J, H, K_s$  (2MASS),  $W1$  (WISE), and  $i, z, y$  (Pan-STARRS), which we used to compute the corresponding apparent color indices. We did not use WISE  $W2$ -band data (with a effective wavelength of  $\lambda = 4.6 \mu m$ ) because of an extinction peak in the vicinity of  $\lambda = 4.5 \mu m$  [33], which evidently does not fit the supposed monotonic power-law decrease of extinction with wavelength. Table I lists the effective wavelengths of the photometric passbands employed.

To determine the intrinsic (true) color indices, we used theoretical isochrones [11–13] and the ZAMS determined with the initial mass function of Kroupa [14]. We fitted the distribution of color excesses  $E(r - \lambda_i) = (r - \lambda_i)_{vis} - (r - \lambda_i)_0$  for stars in each cluster by a Gaussian function to determine the average  $E(r - \lambda_i)$  values.

We then plotted for each cluster the dependence of the average  $E(r - \lambda_i)$  color excess on effective wavelength  $\lambda_{eff}(i)$ . In the near infrared this dependence can be described by a function of the following form [34]:

$$E(r - \lambda) = a + b \cdot \lambda^{-\alpha} \quad (3)$$

The color excess  $E(r - \lambda)$  in the limit  $\lambda \rightarrow \infty$  tends to  $A_r$  – the total extinction in the  $r$ -band filter, i.e., solving equation (3) yields  $A_r = a$ . Given the earlier determined color excess  $E(r - i)$  (see Section II A above), we determine the parameter  $R_r = \frac{A_r}{E(r-i)}$  of the extinction law.

To determine the extinction law toward each cluster, we selected stars lying in the vicinity of the minimum in the  $(r-i, H_\alpha index)$  diagram. In the case of 14 clusters

out of 108 we found no or too selected stars with available  $W1$ -band magnitude, and performed all subsequent computations for the remaining 94 open clusters. We refined the membership status of selected stars based on the proper motions from Gaia DR2 catalog, which became publicly available at this stage of our study. We fitted the distribution of stars in the  $(\mu_\alpha, \mu_\delta)$  plane by a two-component Gaussian:

$$f = \frac{1}{2\pi\sigma_\alpha\sigma_\delta\sqrt{1-k^2}} \cdot \exp\left(-\frac{1}{2(1-k^2)}\left[\frac{(\mu_\alpha^i - \mu_\alpha)^2}{\sigma_\alpha^2} - k\frac{2(\mu_\alpha^i - \mu_\alpha)(\mu_\delta^i - \mu_\delta)}{\sigma_\alpha\sigma_\delta} + \frac{(\mu_\delta^i - \mu_\delta)^2}{\sigma_\delta^2}\right]\right), \quad (4)$$

where  $\mu_\alpha, \sigma_\alpha, \mu_\delta, \sigma_\delta$  - are the means and standard deviations of the corresponding distributions and  $k$  is the correlation coefficient. The probability contours have the form of ellipses described by equation:

$$\frac{(\mu_\alpha^i - \mu_\alpha)^2}{\sigma_\alpha^2} - k\frac{2(\mu_\alpha^i - \mu_\alpha)(\mu_\delta^i - \mu_\delta)}{\sigma_\alpha\sigma_\delta} + \frac{(\mu_\delta^i - \mu_\delta)^2}{\sigma_\delta^2} = const \quad (5)$$

The  $const = 9$  ellipse defines the area of the scatter of proper motions of individual stars within  $3\sigma$  of the mean values, and it is these stars that we use to derive the extinction law, which we approximated via non-linear least-squares fitting. After the first approximation we rejected stars lying outside the  $3\sigma$  and repeated the procedure. We used the inferred  $\mu_\alpha, \sigma_\alpha, \mu_\delta, \sigma_\delta$  values to estimate the components of the average proper motion of the cluster and their standard errors.

We then determined the parameters  $R_r$  and  $\alpha$  of the interstellar extinction law from the data of identified cluster members and used the inferred  $R_r$  value to compute the photometric distance to the cluster in pc and the corresponding photometric parallax. We also computed the weighted mean trigonometric parallaxes of the clusters by averaging Gaia DR2 individual of cluster members.

### III. RESULTS

We list the results in Table II. Column 1 gives the name of the cluster; columns 2 and 3, the photometric distance to the cluster and its standard error in pc, respectively. Columns 4 and 5 give the photometric parallax of the cluster computed from the photometric distance and its standard error, respectively. Columns 6 and 7 give the astrometric (trigonometric) parallax of the cluster computed from Gaia DR2 data and its standard error, respectively. Column 8 gives the logarithm of the cluster age in Myr; columns 9 and 10 give the extinction-law parameter  $R_r$  and its standard error, respectively; columns 11 and 12 give the total extinction in the  $r$  band and its standard error, respectively; columns 13 and 14 give

the exponent  $\alpha$  from equation (3) and its standard error, respectively. Columns 15 and 16 give the average proper-motion component of the cluster along right ascension and its standard error in mas/yr, respectively. Columns 17 and 18 give average proper-motion component of the cluster along declination and its standard error in mas/yr, respectively. The full version of Table II is available in electronic form at:

[www.sai.msu.ru/groups/cluster/cl/iphas\\_ocl](http://www.sai.msu.ru/groups/cluster/cl/iphas_ocl)

Figure 3 compares the photometric and Gaia DR2 astrometric parallaxes of the clusters studied. As is evident from the figure, astrometric parallaxes are systematically smaller than photometric parallaxes. The dashed line shows the equality diagonal and the solid line shows the linear relation found by minimizing the function of the following form via the simplex method:

$$\chi^2 = \sum_{i=1} \frac{(\pi_{gaia,i} - a \cdot \pi_i - b)^2}{\sigma_{gaia,i}^2 + a^2 \cdot \sigma_i^2}, \quad (6)$$

where the constants are equal to  $a_{opt} = 0.983 \pm 0.025$  and  $b_{opt} = -44.6 \pm 8.9$  microarcseconds. We estimated the errors by constructing the section of surface  $\chi^2(a, b)$  by the plane  $\chi^2 = \chi^2(a_{opt}, b_{opt}) + 1$ . Hence our photometric distance scale (and the scale of photometric parallaxes) of clusters is consistent with the distance scale implied by Gaia DR2 trigonometric parallaxes (the coefficient  $a_{opt} = 0.983 \pm 0.025$  does not differ from unity within the quoted errors), and the systematic error of the scale of Gaia DR2 trigonometric parallaxes is of about  $-44.6 \pm 8.9$  microarcseconds (measured trigonometric parallaxes are, on the average, underestimated by this amount).

In their guidelines for using Gaia DR2 parallaxes Luri et al. [35] admit a zero-point offset of 30 microarcseconds. Zinn et al. [36] estimate the Gaia DR2 parallax zero-point offset to be  $52.8 \pm 3.4$  and  $50.2 \pm 3.5$  microarcseconds from the data for red-giant branch and red-clump stars, respectively. Riess et al. [38] found the offset to be  $46 \pm 13$  microarcseconds from their analysis of bright Galactic Cepheids. Like in this study, Gaia DR2 parallaxes are always found to be systematically underestimated.

Figure 4 shows the distribution of inferred values of parameter  $R_r$ , which characterizes interstellar extinction law. The mean value  $\langle R_r \rangle = 3.99 \pm 0.04$  differs significantly (albeit slightly) from the value implied by the “standard” law of Cardelli et al. [30] ( $R_r = 3.88$ ), agrees better with the extinction law of O’Donnell [31] ( $R_r = 4.07$ ), both with  $R_V = 3.1$ . Note the broad scatter of the distribution in Fig. 4 with a standard deviation of  $\sigma_{R_r} = 0.35$ .

Figure 5 shows the distribution of the clusters studied projected onto the Galactic plane in polar coordinates. The color of the circles corresponds to the inferred  $R_r$  value: the darker color, the higher  $R_r$ . Extinction law can be seen to vary conspicuously both with distance and direction.

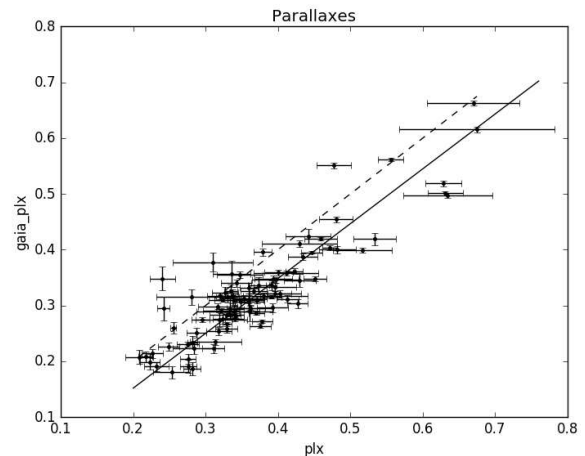


FIG. 3: Comparison of photometric and Gaia DR2 astrometric parallaxes. The dashed line shows the equality diagonal and the solid line shows the inferred linear relation.

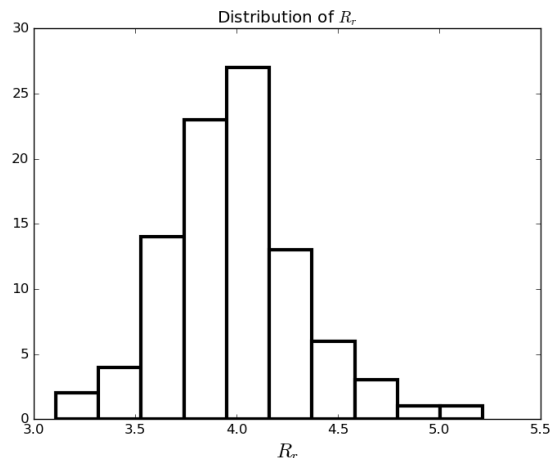


FIG. 4: Distribution of extinction-law parameter  $R_r$  in the fields of 94 open clusters studied.

In their review Matsunaga et al. [39] point out that the studies performed before 1995 yielded exponents  $\alpha$  (equation (3)) in the 1.6 – 1.8 interval, whereas later estimates of  $\alpha$  obtained by different authors span from 0.8 to 2.6 [40]. The exponents  $\alpha$  found in this work span an even broader interval from 0.74 to 4.01 (see Fig. 6) with a mean and standard deviation equal to  $\langle \alpha \rangle = 2.05$  and  $\sigma_\alpha = 0.58$ , respectively.

Figure 7 shows the distribution of the difference between the cluster proper-motion component in right ascension computed using the Sanders method in Section II B and the cluster proper motions determined from Gaia DR2 data in Section II C. Figure 8 shows the corresponding difference for the proper-motion components in declination. The mean values and standard deviations are equal to  $\langle \Delta\mu_\alpha \rangle = -1.036 \pm 0.088$  mas/yr,  $\sigma_{\Delta\mu_\alpha} = 0.998 \pm 0.088$  mas/yr and  $\langle \Delta\mu_\delta \rangle = 0.347 \pm$

TABLE II: Parameters of open clusters

Cluster	$D$	$\sigma_D$	$\pi$	$\sigma_\pi$	$\pi_{gaia}$	$\sigma_{\pi_{gaia}}$	$\log(t)$	$R_r$	$\sigma_{R_r}$	$A_r$	$\sigma_{A_r}$	$\alpha$	$\sigma_\alpha$	$\mu_\alpha$	$\sigma_{\mu_\alpha}$	$\mu_\delta$	$\sigma_{\mu_\delta}$
	pc	pc	mas	mas	mas	mas	Myr							mas/yr	mas/yr	mas/yr	mas/yr
sai13	3035	220	0.329	0.024	0.283	0.005	8.2	3.752	0.048	3.487	0.057	1.934	0.039	-1.610	0.009	-0.056	0.009
sai14	2873	89	0.348	0.011	0.307	0.010	7.6	4.131	0.083	2.666	0.060	1.838	0.085	-1.555	0.072	-0.269	0.053

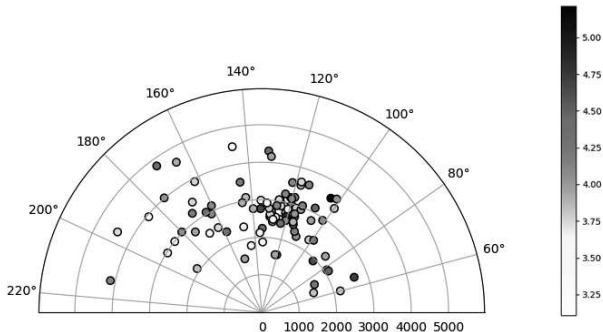


FIG. 5: Distribution of clusters projected onto the Galactic plane. The Sun is at the coordinate origin, the radius gives the heliocentric distance in pc and the angle, the Galactic longitude. The color corresponds to the value of parameter  $R_r$ .

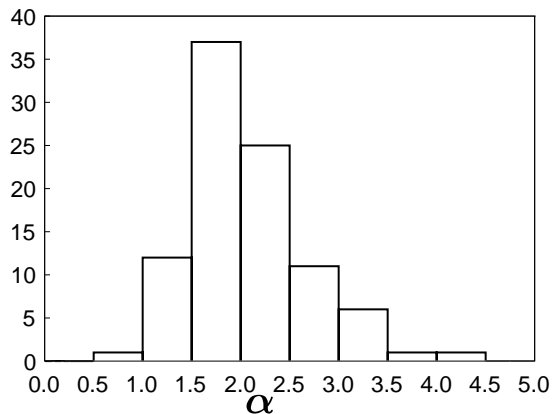


FIG. 6: Distribution of extinction-law parameter  $\alpha$  in the fields of 94 open clusters studied.

$0.090 \text{ mas/yr}$ ,  $\sigma_{\Delta\mu_\delta} = 0.910 \pm 0.091 \text{ mas/yr}$ . Thus the mean differences of proper-motion components prove to be comparable to the estimate of characteristic systematic errors of the UCAC5 catalog, which we used to define our reference frame: according to UCAC5 authors, these systematic errors are within  $0.7 \text{ mas/yr}$  [21]. Table II lists only the average cluster proper motions determined from Gaia DR2 data.

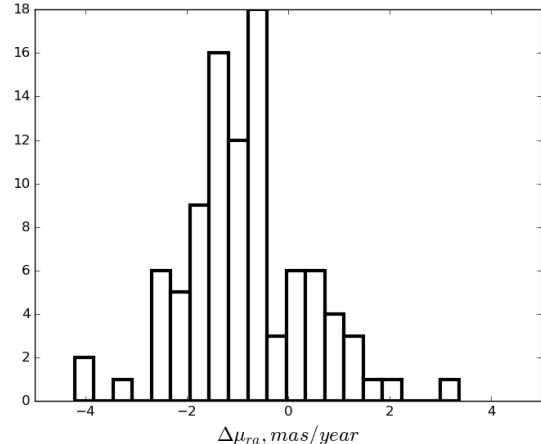


FIG. 7: Comparison of proper motions in right ascension based on positional data from seven catalogs (up to 13 different epochs per star spanning the time interval from 1949 through 2015) with the proper motions based on Gaia DR2 data.

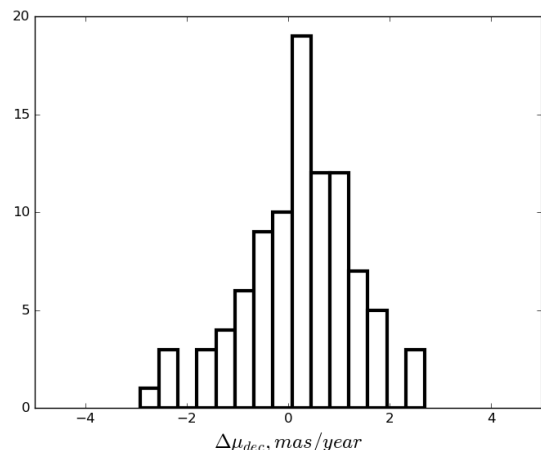


FIG. 8: Comparison of proper motions in declination based on positional data from seven catalogs (up to 13 different epochs per star spanning the time interval from 1949 through 2015) with the proper motions based on Gaia DR2 data.

#### IV. CONCLUSIONS

We determined the photometric distances,  $E_{r-i}$  color excesses (based on IPHAS survey data), ages, the mean Gaia DR2 astrometric parallaxes and proper motions

for almost one hundred Galactic open clusters. We estimated the photometric distances taking into account individual total-to-selective extinction ratios  $A_r/E_{r-i}$  for each cluster, which we determined using the color-difference method applied to IPHAS survey  $r$ -,  $i$ -, and  $H_\alpha$ -band photometry, 2MASS  $J$ -,  $H$ , and  $K_s$ -band photometry, WISE  $W1$ -band photometry, and Pan-STARRS  $i$ -,  $z$ -, and  $y$ -band photometry. The inferred  $R_r$  ratios vary significantly from cluster to cluster, the mean and standard deviation are equal to  $\langle R_r \rangle = 3.99$  and  $\sigma_{R_r} = 0.34$ , respectively. We found our photometric distance scale to agree well with the scale of Gaia DR2 trigonometric parallaxes, which, on the average, are systematically underestimated by  $45 \pm 9$  microarcseconds in good agreement with the results obtained by other authors based on other objects (classical Cepheids, quasars, red-giant and red-clump stars).

### Acknowledgments

This work was supported by the Russian Foundation for Basic Research (grant no. 18-02-00890). This publication makes use of data products from the Two Micron All Sky Survey (2MASS), which is a joint project of the University of Massachusetts and the Infrared Processing and Analysis Center/California Institute of Technology, funded by the National Aeronautics and Space Administration and the National Science Foundation, and of the data products from the Wide-field Infrared Survey Explorer (WISE), which is a joint project of the University of California, Los Angeles, and the Jet Propulsion Laboratory/California Institute of Technology, and NEOWISE, which is a project of the Jet Propulsion Laboratory/California Institute of Technology. WISE and NEOWISE are funded by the National Aeronautics and Space Administration. This publication also makes use of the data obtained as part of the INT Photometric  $H_\alpha$  Survey of the Northern Galactic Plane (IPHAS, [www.iphas.org](http://www.iphas.org)) carried out at the Isaac Newton Telescope (INT) and the data of Pan-STARRS 1 survey, as well as the data from the European Space Agency (ESA) mission *Gaia* (<https://www.cosmos.esa.int/gaia>), processed by the *Gaia* Data Processing and Analysis Consortium (DPAC, <https://www.cosmos.esa.int/web/gaia/dpac/consortium>). Funding for the DPAC has been provided by national institutions, in particular the institutions participating in the *Gaia* Multilateral Agreement.

- 
- [1] A. A. Chemel, E. V. Glushkova, A. K. Dambis, et al., *Astrophysical Bulletin* **73**, 162 (2018)
- [2] G. Barentsen, H. J. Farnhill, J. E. Drew, et al., *Monthly Notices Royal Astron. Soc.* **444**, 3230 (2014)
- [3] J. E. Drew, R. Greimel, I. M. Irwin, et al., *Monthly Notices Royal Astron. Soc.* **362**, 753 (2005)
- [4] A. K. Dambis, E. V. Glushkova, L. N. Berdnikov, et al., *Monthly Notices Royal Astron. Soc.* **465**, 1505 (2017)
- [5] W. S. Dias, B. S. Alessi, J. R. Moitinho, et al., *Astron. and Astrophys.* **389**, 871 (2002)
- [6] N. V. Kharchenko, A. E. Piskunov, S. Roeser, et al., *Astron. and Astrophys.* **558**, 53 (2013)
- [7] M.F. Skrutskie, R.M. Cutri, R. Stiening, et al., *Astron. J.* **131**, 1163 (2006)
- [8] Gaia Collaboration, et al., *Astron. and Astrophys.* **595**, 1 (2016)
- [9] Gaia Collaboration, A. G. A. Brown, A. Vallenari, et al., arXiv1804.09365 (2018)
- [10] H. L. Johnson, W. W. Morgan, *Astrophys. J.* **117**, 313 (1953)
- [11] Y. Chen, L. Girardi, A. Bressan, et al., *Monthly Notices Royal Astron. Soc.* **444**, 2525 (2014)
- [12] Y. Chen, A. Bressan, L. Girardi, et al., *Monthly Notices Royal Astron. Soc.* **452**, 1068 (2015)
- [13] J. Tang, A. Bressan, P. Rosenfield, et al., *Monthly Notices Royal Astron. Soc.* **445**, 4287 (2014)
- [14] P. Kroupa, *Monthly Notices Royal Astron. Soc.* **322**, 231 (2001)
- [15] A. Henden, U. Munari, *Contribution of the Astronomical Observatory Skalnaté Pleso* **43**, no. 3, 518 (2014)
- [16] A. Henden, M. Templeton, D. Terrell, et al., *VizieR Online Data Catalog*, II/336 (2016)
- [17] T. Naylor, R. D. Jeffries, *Monthly Notices Royal Astron. Soc.* **373**, 1251 (2006)
- [18] R. D. Jeffries, J. M. Oliveira, T. Naylor, et al., *Monthly Notices Royal Astron. Soc.* **376**, 580 (2007)
- [19] N. I. Mayne, T. Naylor, S. P. Littlefair, et al., *Monthly Notices Royal Astron. Soc.* **375**, 1220 (2007)
- [20] D.G. Monet, S.E. Levine, B. Canzian, et al., *Astron. J.* **125**, 984 (2003)
- [21] N. Zacharias, C. Finch, and J. Flouard, *Astron. J.* **153**, 166 (2017)
- [22] E.L. Wright, P.R.M. Eisenhardt, A.K. Mainzer, et al., *Astron. J.* **140**, 1868 (2010)
- [23] A. Mainzer, T. Grav, J. Bauer, et al., *Astrophys. J.* **743**, 156 (2011)
- [24] N. Zacharias, C. Finch, J. Subasavage, et al., *Astron. J.* **150**, 101 (2015)
- [25] F. Bonnarel, P. Fernique, O. Bienaymé, et al., *Astron. and Astrophys. Suppl.* **143**, 33 (2000)
- [26] M. B. Taylor, *Astronomical Society of the Pacific Conference Series* **351**, 666 (2006)
- [27] M. B. Taylor, *Astronomical Society of the Pacific Conference Series* **347**, 29 (2005)
- [28] G. Riccio, M. Brescia, S. Cavuoti, *Publ. Astron. Soc. Pacific* **129**, 024005 (2017)
- [29] W. D. Sanders, *Astron. and Astrophys.* **14**, 226 (1971)
- [30] J. Cardelli, G. Clayton, J. Mathis, *Astrophys. J.* **345**, 245 (1989)
- [31] J. O'Donnell, *Astrophys. J.* **422**, 158 (1994)
- [32] E. L. Fitzpatrick, D. Massa, *Astrophys. J.* **663**, 320 (2007)
- [33] G. A. Gontcharov, *Astrophysics* **59**, 548 (2016)
- [34] J. E. Drew, E. Gonzalez-Solares, R. Greimel, et al., *Monthly Notices Royal Astron. Soc.* **440**, 2036 (2014)
- [35] X. Luri, A. G. A. Brown, L. M. Sarro, et al., *Astron. and Astrophys.* in press (2018), arXiv180409376
- [36] J. C. Zinn, M. H. Pinsonneault, D. Huber, et al., arXiv:1805.02650
- [37] M. H. Pinsonneault, Y. P. Elsworth, J. Tayar, et al., arXiv:1804.09983
- [38] A. G. Riess, S. Casertano, W. Yuan, et al., *Astrophys. J.* in press (2018), arXiv:1804.10655
- [39] N. Matsunaga, G. Bono, X. Chen, et al., *Space Science Reviews* **214**, 36 (2018)
- [40] T. J. T. Moore, S. L. Lumsden, N. A. Ridge, et al., *Monthly Notices Royal Astron. Soc.* **359**, 589 (2005)